ChemPubSoc Europe
DOI: 10.1002/chem.201800517
CHEMISTRY A European Journal Minireview

Transmutation

Electronic Transmutation (ET): Chemically Turning One Element into Another

Xinxing Zhang,*[a] Katie A. Lundell,[b] Jared K. Olson,[b] Kit H. Bowen,*[c] and Alexander I. Boldyrev*[b]

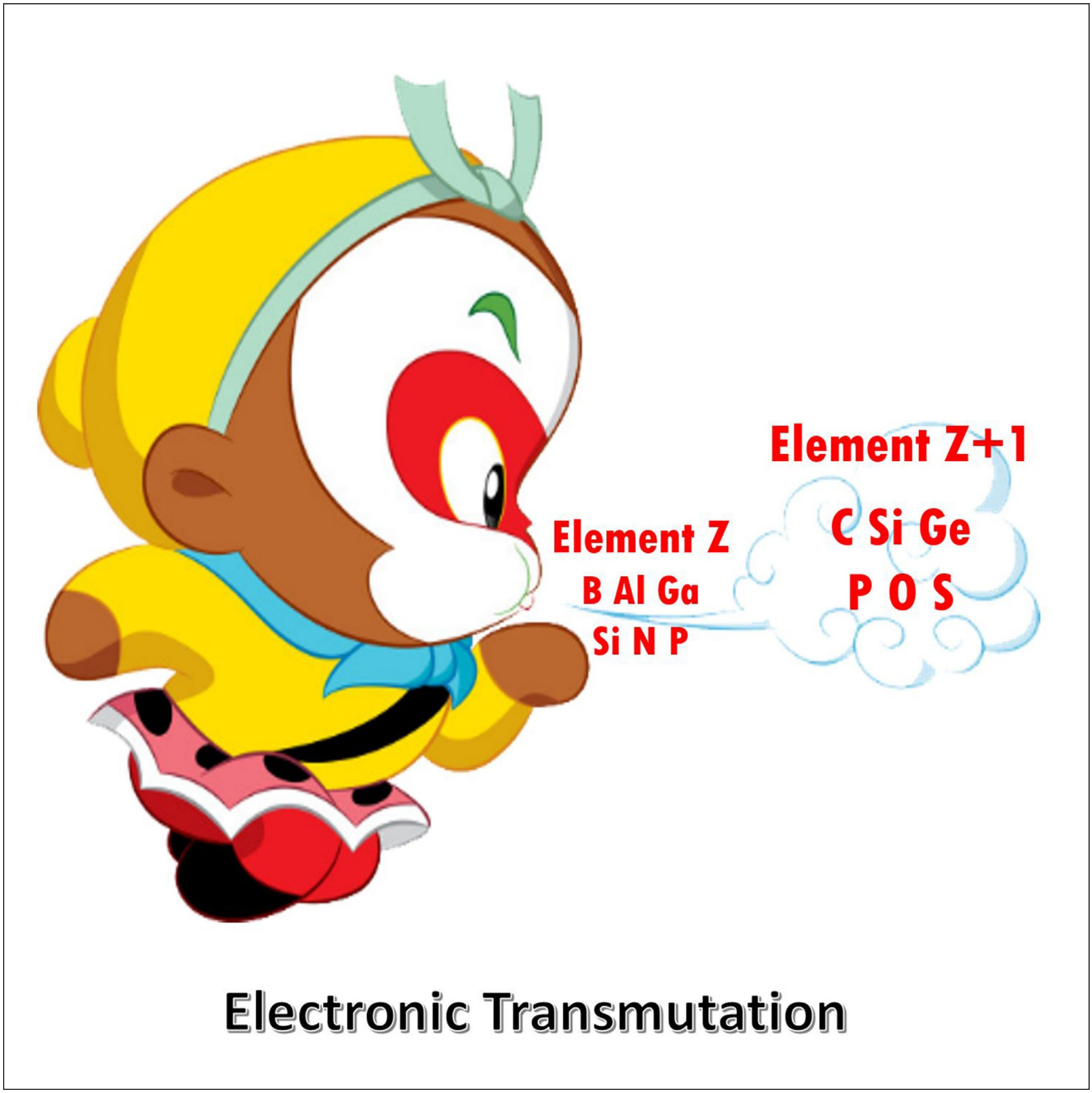

Abstract: The concept of electronic transmutation (ET) depicts the processes that by acquiring an extra electron, an element with the atomic number Z begins to have properties that were known to only belong to its neighboring element with the atomic number Z+1. Based on ET, signature compounds and chemical bonds that are composed of certain elements can now be designed and formed by other electronically transmutated elements. This Minireview summarizes the recent developments and applications of ET on both the theoretical and experimental fronts. Examples on the ET of Group 13 elements into Group 14 elements, Group 14 elements into Group 15 elements, and Group 15 elements into Group 16 elements are discussed. Compounds and chemical bonding composed of carbon, silicon, germanium, phosphorous, oxygen and sulfur now have analogues using transmutated boron, aluminum, gallium, silicon, nitrogen, and phosphorous.

Introduction

Despite the success of the valence-isoelectronic concept in many examples of predicting reactivity, structures and existence of compounds, such a simple electron counting rule can nevertheless easily fail. For instance, being valence-isoelectronic to benzene (C_6H_6), the planar D_{6h} silabenzene molecule Si_6H_6 is not even a minimum on its potential energy surface.[1] The deformation from this planar structure to its real global minimum is attributable to the pseudo-Jahn–Teller effect. In view of this, a stricter and narrower electronic transmutation (ET) concept[2] was proposed in 2012, stating that by acquiring an electron, a certain element with the atomic number Z begins to behave similarly as its neighboring element Z+1. For example, the transmutated boron, B^-, may well be functioning similarly to carbon. The similarities between the transmutated element Z and the targeted element Z+1 could range from the chemical bonding they possess to the geometries of the compounds they form, so that many key features that were thought only belong to element Z+1 can now belong to element Z. Alchemists once spent great efforts in transmutating common elements into precious others, which now we know is not possible merely with chemistry, but based on ET, the element Z can now be chemically "turned into" element Z+1. After the proposal of the ET concept, a plethora of successful examples, including the transmutation of Groups 13, 14, and 15 elements into Group 14, 15, and 16 elements, have been reported.[2–18] In this Minireview, we will summarize these examples on both the theoretical and experimental fronts, and outlook for wider applications and future research directions of this new concept.

[a] *Prof. Dr. X. Zhang*
Collaborative Innovation Center of Chemical Science and Engineering
College of Chemistry, Nankai University
Tianjin 300071 (P. R. China)
E-mail: idea.then.diligence@gmail.com

[b] *K. A. Lundell, Dr. J. K. Olson, Prof. Dr. A. I. Boldyrev*
Department of Chemistry and Biochemistry
Utah State University
0300 Old Main Hill, Logan, UT, 84322-0300 (USA)
E-mail: a.i.boldyrev@usu.edu

[c] *Prof. Dr. K. H. Bowen*
Departments of Chemistry and Material Science
Johns Hopkins University
Baltimore, MD, 21218 (USA)
E-mail: kbowen@jhu.edu

The ORCID identification number(s) for the author(s) of this article can be found under https://doi.org/10.1002/chem.201800517.

1. Electronic Transmutation of Group 13 Elements into Group 14 Elements

Group 13 elements, such as boron,[19] aluminum,[20] and gallium,[21] are well known to form clustered compounds through multicenter bonding, which is largely due to their electron-deficient (s^2p^1 electron configuration) nature. The simplest examples are the diborane (B_2H_6),[22] dialane (Al_2H_6),[23] and digallane (Ga_2H_6)[24] molecules, where each of the two bridge hydrogen atoms participates in forming a 3-center 2-electron (3c–2e) M-H_{bridge}-M (M=B, Al, Ga) bond. Rather distinct from the Group 13 elements, Group 14 elements such as carbon, silicon, and germanium usually form chain or ring compounds as a result of sp^n ($n=1$, 2, 3) hybridizations. With the difference of only one electron, Group 13 and 14 elements behave very differently in chemical bonding and the compounds they can form. In this section, we discuss the theoretical and experimental advances of the electronic transmutation of Group 13 elements into Group 14 elements, where the former yield similar chemical bonding and compounds as the latter after transmutation.

1.1. ET of boron into carbon

It is well-known that carbon forms a large variety of hydrocarbons, including aromatic arene, alkane, alkene, and alkyne-based compounds that feature chain (homocatenation) or ring structures. Boron hydrides, or boranes, on the other hand, prefer clustered structures. In order to satisfy the octet rule, the insufficient electrons in boron lead to the formation of 3c–2e bonds, based on which an extension to molecular orbital (MO) theory was developed, known as the polyhedral skeletal electron pair theory (PSEPT) or simply Wade–Mingos rules.[19] In this section, we present the successful examples of homocatenated and aromatic boron compounds when boron is electronically transmutated into carbon.

We first discuss the theoretical predictions of homocatenated boron hydrides where the ET concept was firstly proposed.[2] Alkanes follow the molecular formula C_nH_{2n+2}, suggesting that their boron analogues should have the formula of

$(B_nH_{2n+2})^{n-}$, in which each boron atom obtains one negative charge to resemble carbon. These negative charges can be provided by certain electron donors, preferably by alkali metals such as Li, so the first obvious example is the BH_4^- kernel in the $LiBH_4$ salt, which is isoelectronic and isostructural to CH_4, and already commercially available. Here we focus on the homocatenation of boron, and $Li_2B_2H_6$ seems to be a simple candidate to start with. However, the B–Li, H–Li, and B–H bond dissociation energies are not too far away from each other,[25] one would expect a relatively flat potential energy surface and many possible isomers that are close in energy for this molecule, which makes a thorough, unbiased geometrical search indispensable but very expensive in order to find the real global minimum. Here we present the detailed calculation methods used in reference [2] in order to set an example for the search of the global minimum of electronically transmutated molecules. The computational methods for other ET molecules in the rest of this minireview are more or less the same as the case of $Li_2B_2H_6$ unless noted. The search for the global minimum structure of the $Li_2B_2H_6$ molecule was performed using the Coalescence Kick program written by Averkiev.[26] Initially these calculations were performed at a relative low/cheap level of theory (B3LYP/3–21G[27]) to search for a large quantity of isomers, and those lowest energy isomers ($\Delta E < 60$ kcal mol^{-1}) were then reoptimized and frequencies were calculated at B3LYP/6–311++G**[28] and CCSD(T)/6–311++G**[29] and single point calculations were performed using the RCCSD(T)/aug-cc-pVXZ levels of theory (X = D and T).[30] The final relative energies were obtained through extrapolation of total energies at the CCSD(T) level of theory to the complete basis set limit (CBS) using the Truhlar formula[31] (CCSD(T)/CBS//CCSD(T)/6–311++G**) and corrected for zero-point energies calculated at CCSD(T)/6–311++G**. Chemical bonding analysis (B3LYP/6–311++G**) was performed using the AdNDP method.[32] All calculations were done using GAUSSIAN 03 and GAUSSIAN 09[33] software packages. Molekel 5.4.0.8 was used for MO visualization,[34] and MOLDEN t3.4[35] was used for molecular structure visualization.

Figure 1 A presents the global minimum of $Li_2B_2H_6$, which contains one 2c–2e B–B σ-bond and six 2c–2c B–H σ-bonds. These σ-bonds are further confirmed by AdNDP analysis (Figure 1 D). From the structure, the B_2H_6 kernel is indeed very similar to the hydrocarbon analog, ethane. However, the interaction between the Li atoms and the B_2H_6 kernel appears to be critical to determine the existence of electronic transmutation. Calculated effective charges are $+0.94|e|$ on each Li atom and $-1.88|e|$ on the B_2H_6 kernel. Thus, the interaction between the Li and the B_2H_6 kernel is ionic, and the B_2H_6 moiety is

Xinxing Zhang obtained his B.S. in chemistry at Fudan University in Shanghai, China (2009), and his PhD at the Johns Hopkins University in the Kit Bowen research group (2015). Since 2016, he has been working as a postdoctoral scholar at Caltech in the J. L. Beauchamp research group. His research interests cover gas phase cluster reactivity and spectroscopy, as well as the physical chemistry and biochemistry at the air–water interfaces. He started his independent research career as a professor at Nankai University, Tianjin, China, in 2018.

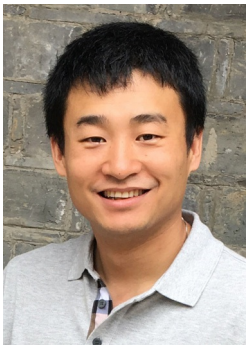

Katie Lundell received her B.S. in chemistry and biochemistry at Idaho State University in Pocatello, Idaho (2015). Since 2016 she has been a graduate student in the Alex Boldyrev research group. Her research interests are the study of electronic transmutations and development of new chemical bonding models in clusters.

Jared K. Olson received his B.S. (2002) and M.S. (2004) in physics from the University of Utah, MBA (2006) from Westminster College, and Ph.D. (2010) in Physical Chemistry from Utah State University. He is currently a Sr. Program Manager in the Propulsion Systems Division at Orbital ATK. His scientific interest is in chemical bonding models, the rational design of new molecules, and propulsion systems technology.

Kit H. Bowen, Jr. received his B.S. in chemistry at the University of Mississippi (1970), and his M.S. (1973) and Ph.D. (1977) in chemistry at Harvard University. He was also an NSF postdoc at Harvard University. Dr. Bowen is now the E. Emmet Reid Professor of Chemistry at the Johns Hopkins University. His research utilizes negative ion photoelectron spectroscopy and surface deposition techniques both of which are applied to size-selected cluster anions.

Alexander I. Boldyrev received his B.S./M.S. in chemistry from Novosibirsk University (1974), his Ph.D. in physical chemistry from Moscow State University (1978), and his Dr. Sci. in chemical physics from Moscow Physico-Chemical Institute (1987). He is currently a Professor at the Department of Chemistry and Biochemistry at Utah State University. His current scientific interest is the development of new chemical bonding models for clusters, molecules, solid state materials, novel two-dimensional materials and other chemical species, where conventional chemical bonding models are not applicable.

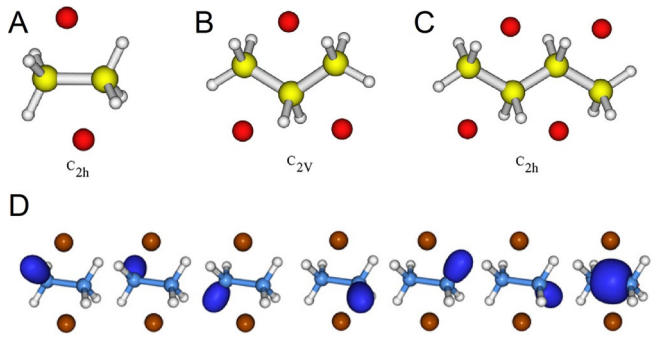

Figure 1. Calculated global minimum structures of $Li_2B_2H_6$ (A), $Li_3B_3H_8$ (B), $Li_4B_4H_{10}$ (C), and the chemical bonding of $Li_2B_2H_6$ recovered by the AdNDP analysis (D).

indeed in the form of $B_2H_6^{2-}$. In other words, electronic transmutation has occurred.

From $Li_2B_2H_6$ to $Li_3B_3H_8$ and $Li_4B_4H_{10}$, the expensiveness of the global minimum search increases exponentially with the number of atoms involved, hence, the authors did not attempt to search for the global minimum, instead, they examined whether or not the propane- and *n*-butane-shaped molecules were local minima on their potential surfaces. The structures in Figure 1B and 1C indeed display similar structures as propane and n-butane, manifesting the success of the electronic transmutation in the homocatenation of boron hydrides.

We next discuss the electronically transmutated aromatic boron hydrides, analogues of arenes. Benzene (C_6H_6), cyclopentadienide ($C_5H_5^-$), tropylium ($C_7H_7^+$),[36] and naphthalene ($C_{10}H_8$) are planar aromatic hydrocarbons, following the $4n+2$ aromaticity rule. Closo-boranes,[19] $B_nH_n^{2-}$ or $B_nH_{n-2}^{4-}$, feature polyhedral structures (Figure 2C, F, I, L). By donating negative charges to these 3-dimensional closo-boranes, is it possible to "flatten" them into aromatic 2-dimensional arene analogues? Alexandrova and Boldyrev[3] examined the calculated global minima of $B_6H_6Li_6$ (Figure 2A, B), $B_5H_5Li_6$ (Figure 2D, E), $B_7H_7Li_6$ (Figure 2G, H), and $B_{10}H_8Li_{10}$ (Figure 2J, K), which are isoelectronic to C_6H_6, $C_5H_5^-$, $C_7H_7^+$ and $C_{10}H_8$, respectively. All of these B_nH_n kernels are planar, and the formal negative charges on B_nH_n revealed by natural bond orbital (NBO) analysis[37] are close to *-n*, indicating that boron atoms in these molecules are transmutated into carbon. More importantly, are these $B_nH_n^{n-}$ kernels aromatic? Nucleus-independent chemical shifts (NICS) indices were introduced by Schleyer[38] as a simple probe for aromaticity. The NICS index at the center of the $B_6H_6^{6-}$ kernel is −7.2 ppm, very close to that of benzene (−8.0 ppm) calculated at the same level of theory. NICS indices for other species are −2.0 ppm for $B_5H_5Li_6$, −93.2 ppm for $B_7H_7Li_6$, and −54.2 ppm for $B_{10}H_8Li_{10}$, providing evidence of their aromaticity. Figure 2M presents the three aromatic π-molecular orbitals of $B_6H_6Li_6$, all of which are similar to that of benzene.

Similarly, Tiznado and co-workers[4] theoretically investigated the $Li_6(BH)_5$ and $Li_7(BH)_5^+$ clusters, and discovered that the $B_5H_5^{6-}$ kernels in the global minima are the transmutated analogues of cyclopentadienide ($C_5H_5^-$). Solá, Teixidor and co-workers[5] examined the intrinsic relationship between the

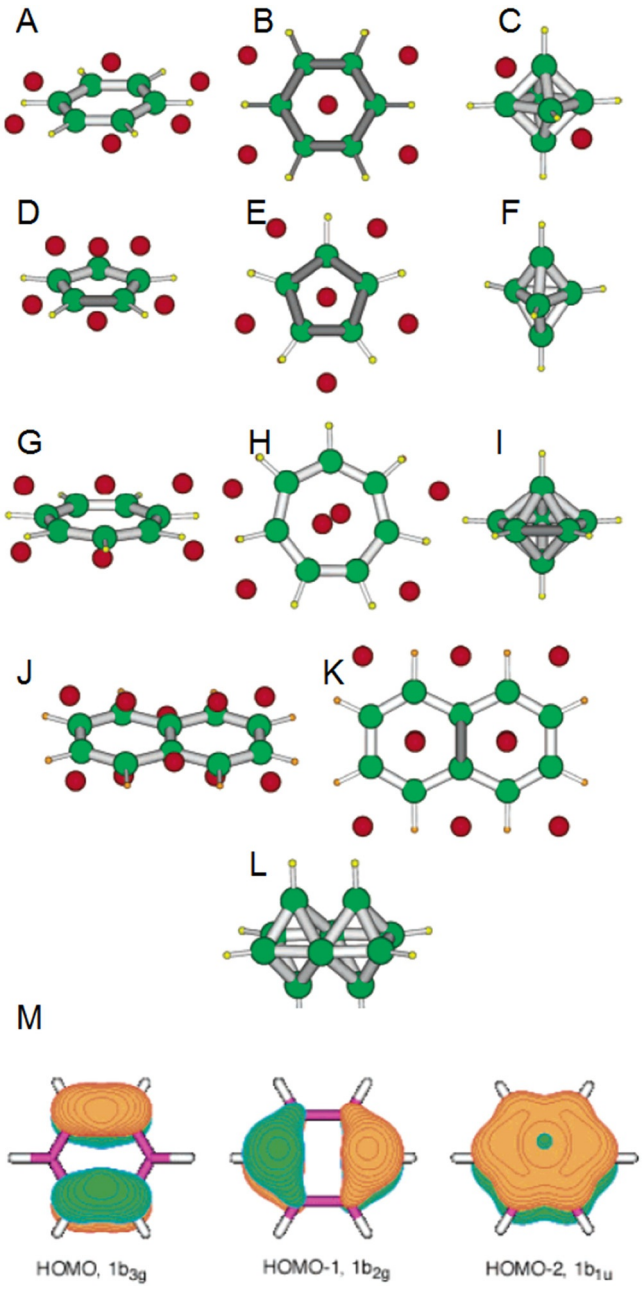

Figure 2. Optimized structures of $B_6H_6Li_6$ (D_{2h},^1A_g), side view (A); $B_6H_6Li_6$ (D_{2h},^1A_g), front view (B); $B_6H_6Li_2$ (D_{3d},$^1A_{1g}$) (C); $B_5H_5Li_6$ (C_s,$^1A'$), side view (D); $B_5H_5Li_6$ (C_s,$^1A'$), front view (E); $B_5H_5^{2-}$ (D_{3h},$^1A_1'$) (F); $B_7H_7Li_6$ (C_1,^1A), side view (G); $B_7H_7Li_6$ (C_1,^1A), front view (H); $B_7H_7^{2-}$ (D_{5h},$^1A_1'$) (I); $B_{10}H_8Li_{10}$ (D_{2h},^1A_g), side view (J); $B_{10}H_8Li_{10}$ (D_{2h},^1A_g), front view (K); and $B_{10}H_8^{4-}$ (D_{2h},^1A_g) (L). π-molecular orbitals of $B_6H_6Li_6$ (D_{2h},^1A_g) (M).

Wade–Mingos rule and $(4n+2)\,\pi$ Hückel rule using the electronic confined space analogy (ECSA) method, in which the electronic transmutation concept turned out to be a key factor.

We next present two extreme examples of transmutated boron, the aromatic 2D boron films, which can be viewed as the analogue of graphene. Graphene is one of the allotropes of carbon consisting of a single planar layer of carbon atoms arranged in a hexagonal lattice.[39] Graphene's boron "cousin"

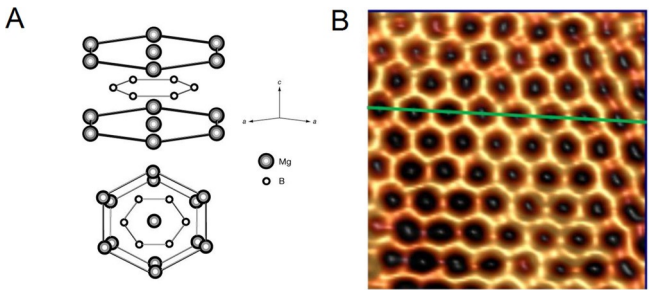

Figure 3. (A) Crystal structure of MgB_2; (B) Scanning tunnelling microscopy image of a graphene-like borophene sheet on an Al substrate.

needs to have the stoichiometry of B_n^{n-}. Using powder X-ray diffraction, Akimitsu and co-workers confirm that there are extraordinary 2D layers of honeycomb structures composed of boron atoms with Mg atoms located above and below the boron hexagon (Figure 3A) in the well-known high-temperature superconductor MgB_2.[6] The 2D-lattice of boron appears to be structurally the same as graphene. Even though not clearly stated by the authors, a complete charge transfer from Mg to B in the form of $Mg^{2+}B_2^{2-}$ due to the large electronegativity difference between Mg and B can be anticipated, and the electronic transmutation principle apparently plays a key role in forming this 2D structure. The B_n^{n-} sheet might be the reason for this material's high-temperature superconducting behavior. During the review process of this minireview, the successful preparation of a honeycomb, graphene-like borophene (Figure 3B) by using an Al surface as the substrate and electron donor was reported.[40] The authors point out that nearly one electron charge is transferred to B from Al, which makes a great example of ET in the application of solid state chemistry. Without electron transfer, the 2D boron film on Ag surface otherwise displays very different structure.[41]

1.2. ET of aluminum into silicon

As a result of the development of modern gas-phase spectroscopy techniques, many aluminum hydrides (alanes) have been discovered using the pulsed arc cluster ionization source (PACIS) and characterized using the anion photoelectron spectroscopy method.[20] Without ET, aluminum hydrides prefer polyhedral structures, following the Wade–Mingos rule just like boranes.[20a] Similar to the ET of boron into carbon, the ET of aluminum into silicon also involves electron donation to aluminum to make Al^-.

The first ET example of aluminum is the homocatenation of aluminum hydrides. The stoichiometry $Li_nAl_nH_{2n+2}$ was attempted to theoretically test the viability of ET for aluminum. Figure 4A presents the global minimum structures of $Li_2Al_2H_6$ and $Li_3Al_3H_8$[7] and they do have similar structures as corresponding disilane[42]/ethane and trisilane[42]/propane. Figure 4B shows the chemical bonds of $Li_2Al_2H_6$ revealed by AdNDP, including one Al–Al σ-bond and six Al–H σ bonds, and all of the occupation numbers are more than 1.9|e|, indicating effective single bonds. The natural population analysis (NPA) charges of Li and the Al_2H_6 kernel are +0.89 and −1.77, suggesting an almost

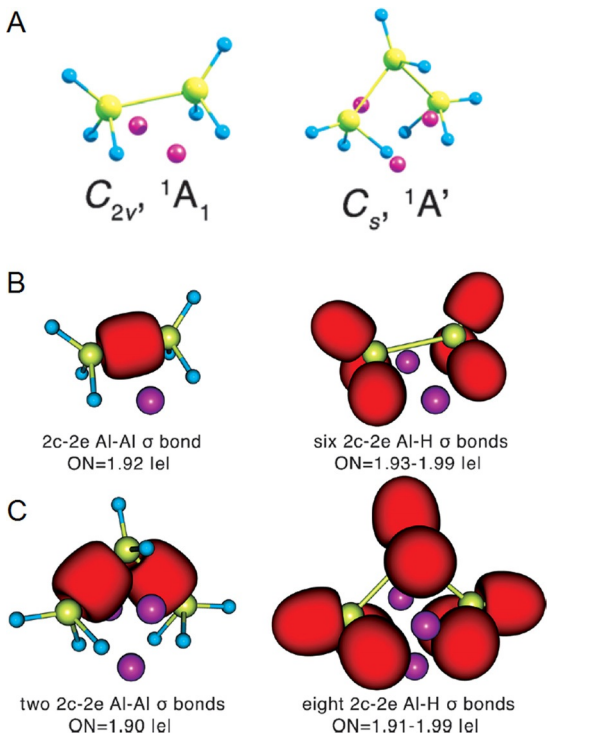

Figure 4. Global minimum structures of $Li_2Al_2H_6$ and $Li_3Al_3H_8$ (A), and the chemical bonds of $Li_2Al_2H_6$ (B) and $Li_3Al_3H_8$ (C) recovered by the AdNDP analyses.

full electron transfer from Li to Al, therefore ET indeed occurs in $Li_2Al_2H_6$. Figure 4C exhibits the chemical bonds of $Li_3Al_3H_8$, including two Al–Al σ single bonds and eight Al–H σ single bonds, and all the occupation numbers are more than 1.9|e|, too. The natural population analysis (NPA) charges of Li and the Al_3H_8 kernel are +0.86 and −2.60, manifesting that ET is also present in this case. For the first time it has been shown that ET enables aluminum atoms to homocatenate with the formation of silane/alkane-like species.

To experimentally investigate the existence of these exotic homocatenated aluminum hydrides in the gas phase, it is better to study them in the form of ions. For the $Li_nAl_nH_{2n+2}$ molecules, one could study the $Li_{n-1}Al_nH_{2n+2}^-$ anion by losing one Li^+ counter ion from $Li_nAl_nH_{2n+2}$. When $n=1$, AlH_4^-, the simplest monosilane/methane analogue, was first examined by anion photoelectron spectroscopy[43] in the gas phase. The vertical detachment energy (VDE) of AlH_4^- is as high as 4.4 eV, indicating that it is very stable. Anion photoelectron spectroscopy is conducted by crossing a mass-selected beam of negative ions with a fixed-frequency photon beam and energy-analysing the resultant photodetached electrons. It is governed by the energy-conserving relationship, $h\nu = EBE + EKE$, in which hν is the photon energy, EBE is the electron binding (transition) energy, and EKE is the electron kinetic energy. The anion photoelectron spectrometer, which has been described previously,[44] consists of one of many kinds of ion sources, a linear time-of-flight mass spectrometer, a mass gate, a momentum decelerator, a pulsed Nd:YAG photodetachment laser, and a magnetic bottle electron energy analyzer. Photoelectron spec-

tra were taken with 193 nm (6.42 eV) photon energy and calibrated against the well-known photoelectron spectrum of Cu^-.[45] The AlH_4^- cluster anions were generated in a pulsed arc cluster ionization source (PACIS). During operation, a pulsed valve backed by 200 psi of UHP hydrogen is opened for about 200 microseconds and fills a region between a copper anode and grounded aluminum cathode. A 30 microseconds long, 180 V pulse is applied to the copper anode that discharges through the hydrogen gas and subsequently vaporizes the aluminum cathode. The combination of free atomic hydrogen and vaporized aluminum is entrained with the remaining molecular hydrogen and carried along a 20 cm flow tube where it reacts, cools, and forms AlH_4^-, which is then extracted and mass-selected before photodetachment.

$Li_2Al_3H_8^-$, the aluminum analogue of trisilane/propane, was also interrogated by anion photoelectron spectroscopy but generated in a different laser vaporization source.[8] Briefly, an aluminum rod was coated by a very thin layer of $LiAlH_4$ powder, and then ablated by a pulsed Nd:YAG laser beam operating at a wavelength of 532 nm. The resulting plasma was cooled by supersonically expanding a plume of helium gas from a pulsed gas valve (backing pressure of ≈100 psi). Negatively charged anions were then extracted into the spectrometer prior to mass selection and photodetachment. Figure 5 A presents the photoelectron spectra of $Li_2Al_3H_8^-$ taken with 355 nm (3.49 eV) and 266 nm (4.66 eV) photon energies. Both spectra have an EBE band (X) starting from ≈2.20 eV and peaking at 2.70 eV. In case of a sufficient Franck–Condon overlap between the ground state of the anion and the ground state of the neutral, the threshold of the first EBE band (≈2.20 eV) should be the electron affinity (EA) of $Li_2Al_3H_8$. The first experimental VDE, the energy difference between an anion and the corresponding neutral species at the geometry of the anion, corresponds to the peak position of the band X, 2.70 eV. The width of the band X suggests an appreciable geometry change between the ground state of $Li_2Al_3H_8^-$ and that of its neutral. In the 266 nm spectrum, a second band (A) at the higher EBE end peaks at 4.32 eV, corresponding to the transition from the ground state of the anion to the first excited state of the neutral molecule. More importantly, can the $Li_2Al_3H_8^-$ cluster maintain the trisilane/propane-like structure after losing the Li^+ counter ion compared to the neutral $Li_3Al_3H_8$? A thorough unbiased theoretical search finds that the global minimum structure of $Li_2Al_3H_8^-$ still possess the chain structure (Figure 5 B), and chemical bond analysis does show that the two Al–Al bonds and the eight Al–H bonds are σ-bonds with occupation numbers more than 1.7 |e|. The vertical electronic transition calculations from the anion to the corresponding neutral match the X and A peaks, indicating that the experimentally observed cluster is indeed the calculated global minimum. NPA charges also show a significant electron transfer from the Li atoms to the Al_3H_8 kernel. The discovery of $Li_2Al_3H_8^-$ in the gas phase makes the first successful experimental example of the homocatenation of aluminum.

The above discussions are the ET of aluminum hydrides into saturated silane/alkane analogues, and an obvious question is that can one generate unsaturated aluminum hydrides with the ET concept, such as an Al=Al double bond in the $Al_2H_4^{2-}$ kernel? Silicon hydrides are known to have homodinuclear double bonds, such as that in the Si_2H_4 molecule. The Al=Al double bond has been otherwise notoriously difficult to synthesize. A stable neutral compound with an Al=Al double bond was synthesized by Inoue and co-workers using bulky ligands very recently.[46] For the gas phase study, the designed ion is $LiAl_2H_4^-$,[9] which was generated and characterized with the same methods as $Li_2Al_3H_8^-$. The measured anion photoelectron spectrum of $LiAl_2H_4^-$ is presented in Figure 6 A, and three EBE bands were observed (X, X′ and X″), among which X

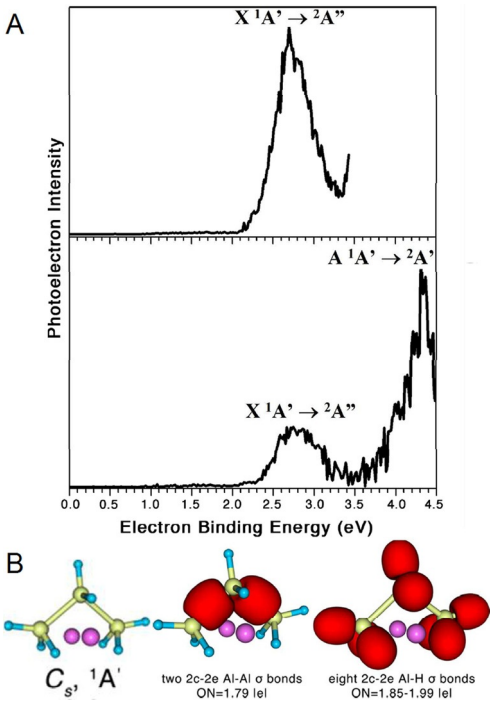

Figure 5. Anion photoelectron spectra of the $Li_2Al_3H_8^-$ anion taken with 355 and 266 nm photons (A) and its global minimum structure and the chemical bonds recovered by the AdNDP analysis (B).

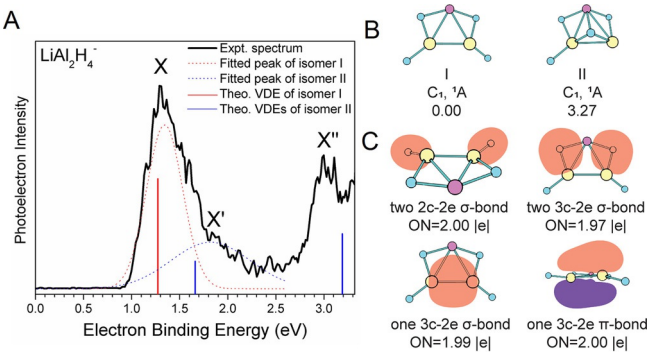

Figure 6. Experimental photoelectron spectrum of $LiAl_2H_4^-$ using 355 nm laser (black line), Gaussian fitting of isomers I and II (red and blue dotted lines), and calculated stick spectra of isomers I and II (red and blue vertical lines) (A); the structures of the two lowest-energy isomers I and II (B), and the chemical bonds of the global minimum structure recovered by the AdNDP analysis (C).

belongs to the global minimum Isomer I, X′ and X″ belong to the second lowest lying Isomer II (Figure 6B). The next question is whether the Al=Al double bond exists in the global minimum structure Isomer I? AdNDP analysis shown in Figure 6C presents two 2c–2e σ-Al–H bonds (ON = 2.00 | e |), two 3c–2e σ-Li-H-Al bonds (ON = 1.97 | e |) (these four bonds are analogous to the σ-Si–H bonds in Si_2H_4), one σ-3c–2e Al-Li-Al bond (ON = 1.99 | e |) (an analogue of the σ-Si–Si bond in Si_2H_4), and one π-Al–Al bond (ON = 2.00 | e |) (an analogue of the π-Si–Si bond in Si_2H_4). In order to claim the presence of the Al=Al double bond, one needs to evaluate how much the lithium atom contributes to the σ and π-3c–2e Al-Li-Al bonds. AdNDP reveals that the σ-3c–2e Al-Li-Al bond (ON = 1.99 | e |) can be seen as one σ-2c–2e Al–Al bond (ON = 1.87 | e |) since the contribution of the lithium atom to this bond is as small as 0.13 | e |. The π-3c–2e Al-Li-Al bond (ON = 2.00 | e |) can be seen as one π-2c–2e Al–Al bond (ON = 1.65 | e |). That gives the (1.87 + 1.65)/2 = 1.76 bond order for Al=Al double bond in the cluster. The optimal bond length between the two Al atoms in $LiAl_2H_4^-$ structure is 2.46 Å (PBE0/6–311 + + G**), which is shorter than the single Al–Al σ-bond (2.59 Å, PBE0/6–311 + + G**) in the H_2AlAlH_2 molecule and the single Al–Al σ-bond (2.55 Å) in the $H_3AlAlH_3^{2-}$ crystal structure.[47] The appreciably shorter Al–Al bond length and the bond order indicate that there is indeed a double bond between the two aluminum atoms. Additionally, the $LiAl_2H_4^-$ cluster is slightly distorted from the planar structure, which is also the case in the Si_2H_4 molecule due to the pseudo Jahn–Teller effect.[48]

1.3. ET of gallium into germanium

Germanium hydrides (germanes), even though not in a large scale, have been synthesized and shown hydrocarbon-like structures.[49] The ET of gallium into germanium enjoys fruitful experimental discoveries.[10–12] Powders of gallium hydride (gallane)-containing compounds, such as $Cs_{10}H[(Ga_3H_8)^{3-}]_3$, $(K_xRb_{1-x})_n[(GaH_2)^-]_n$, $Rb_8[Ga(GaH_3)_4^{5-}]$ and $Rb_n[(GaH_2)^-]_n$ have been synthesized and characterized by X-ray diffraction, where K, Rb and Cs are used as the electron donors. In $Cs_{10}H[(Ga_3H_8)^{3-}]_3$,[10] both ET and the Zintl–Klemm concept[50] are utilized to design the compound, and the $(Ga_3H_8)^{3-}$ kernel is isostructural to propane and Ge_3H_8. In $(K_xRb_{1-x})_n[(GaH_2)^-]_n$[11] and $Rb_n[(GaH_2)^-]_n$,[12] the $[(GaH_2)^-]_n$ polyanions feature polyethylene structures, and in $Rb_8[Ga(GaH_3)_4^{5-}]$,[12] the $Ga(GaH_3)_4^{5-}$ kernel has similar structure as neopentane. In all these examples, each of the Ga atoms obtain one negative charge for the electronic transmutation.

2. Electronic Transmutation of Group 14 Elements into Group 15 Elements

2.1. ET of silicon into phosphorous

In this section, we only discuss one example, the transmutation of silicon into phosphorous. Pure silicon forms the diamond cubic crystal structure.[42] Due to the structure and the high bond energy, silicon is hard. Its neighbour, phosphorus, has several types of allotropes,[42] one of which is the white phosphorus, or simply tetraphosphorus (P_4), existing as molecules composed of four atoms in a tetrahedral structure. In order to transmutate Si into P, theoretical investigations using Li as the electron donor have been attempted.[13,14] Figure 7[14] presents the structural evolution of the global minima and charges on the Si_4 moiety with increasing number of Li atoms in the $Li_nSi_4^-$ series (n = 0–5). According to the ET designing principle, the first Si_4^{4-} kernel mimicking P_4 should occur in the $Li_3Si_4^-$ cluster. Its global minimum indeed shows a tetrahedral Si_4 moiety, and the NPA charge on Si_4 is −3.43 | e |, making it effectively a Si_4^{4-} cluster. Surprisingly, by adding more Li atoms to $Li_3Si_4^-$, the NPA charges on the Si_4 moieties in the $Li_4Si_4^-$ and $Li_5Si_4^-$ clusters remain around −3.5 | e | (Figure 7), suggesting that Si_4 in these clusters have a strong tendency to maintain the ET structure, tetrahedral Si_4^{4-}. The experimental observations of the Si_4^{4-} kernel have been achieved in heavier alkali monosilicides, MSi (M = Na, K, Rb, Cs) in the solid state.[51]

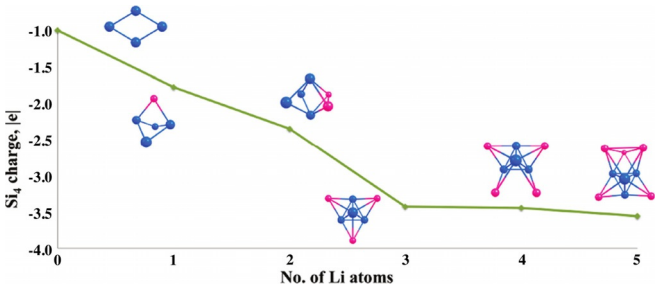

Figure 7. Structural evolution and charge on the Si_4 moiety with increasing number of Li atoms in the $Li_nSi_4^-$ series (n = 0–5).

3. Electronic Transmutation of Group 15 Elements into Group 16 Elements

3.1. ET of nitrogen into oxygen

The ET of nitrogen into oxygen enjoys both the experimental and theoretical developments. In 2001, Kniep et al. synthesized binary diazenides SrN_2 and BaN_2.[15a,b] Schnick et al.[15c] experimentally confirmed the stability of the first alkali diazenide Li_2N_2 under high pressure and high temperature conditions, where Sr, Ba and Li function as the electron donors. In these three examples, the existence of the homonuclear dinitrogen anion N_2^{2-}, an analogue of O_2, are proven by X-ray diffraction, neutron diffraction and infrared spectroscopy. The crystal structures of these examples are displayed in Figure 8. In SrN_2 and BaN_2, each N_2^{2-} kernel is surrounded by an octahedron formed by six Sr^{2+} or Ba^{2+} ions (Figure 8A, 8B), in Li_2N_2, each N_2^{2-} kernel is surrounded by a cube formed by eight Li^+ ions (Figure 8C).

The attempt of finding the ozone analogue, Li_3N_3, was performed theoretically.[15d] The bent ozone-like structure of the N_3^{3-} kernel nevertheless is not the global minimum, but it is only slightly higher in energy than the global minimum. Chemical bond analysis of Li_3N_3 and ozone (Figure 8D, 8E) confirms the similarity in chemical bonding, including two N=N double

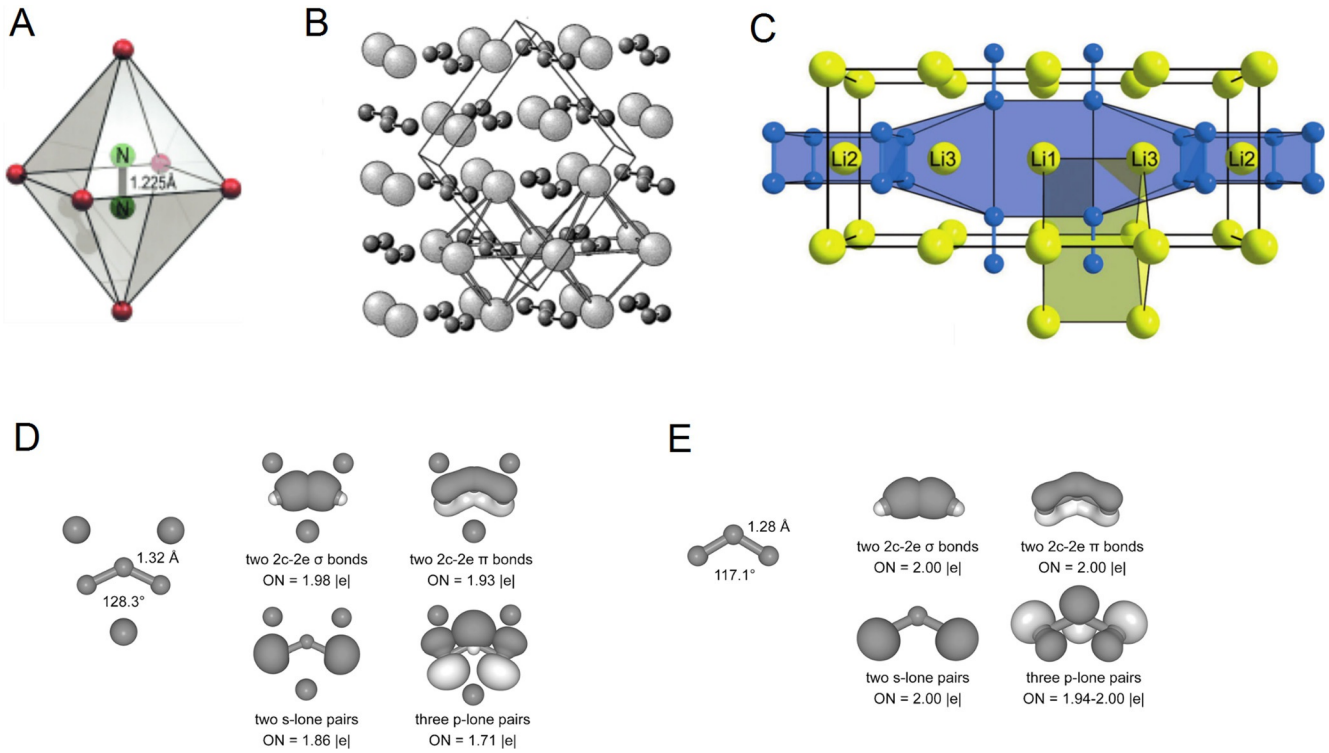

Figure 8. Crystal structures of SrN_2 (A, Sr in red, N in green), BaN_2 (B, Ba in grey, N in black), and Li_2N_2 (C, Li in yellow, N in blue), as well as the chemical bonding of Li_3N_3 (D) and O_3 (E) revealed by the AdNDP analysis.

bonds with occupation numbers (ON) of 1.98 |e| for σ-bonds and 1.93 |e| for π-bonds; one *p*-lone pair on the central nitrogen (ON = 1.72 |e|) and two lone pairs of *s* and *p* type on each side nitrogen atom, with ONs ranging from 1.71 |e| to 1.86 |e|. NBO charge on the N_3 moiety is −2.04 |e|, suggesting significant charge transfer from Li to N.

3.2. ET of phosphorous into sulfur

In search of the transmutated phosphorous, the global minimum search was first performed for Li_xP_x (x = 5–9).[16] Remarkably, inorganic double helix structures were found for all of these clusters. Periodic repetition of the LiP infinite double-helix chain geometry is shown in Figure 9A for illustration. Starting from Li_7P_7 and up to Li_9P_9, the double helices have a similar chemical bonding pattern: effective charges on Li range from +0.8 to +0.9 |e|; there are no Li–P σ-bonds. Six (Li_7P_7), seven (Li_8P_8), and eight (Li_9P_9) P–P σ-bonds with ON = 1.95–1.98 |e| are observed. From this data, it can be concluded that when the bonding between the Li and P atoms is ionic beginning from Li_7P_7 to Li_9P_9, and the double-helix structures are much more favourable relative to other isomers. NBO analysis does not show any significant direct Li–Li covalent bonding. In the graphical representation of double-helix structures, adjacent Li atoms are connected to make the double-helix structure look more apparent. The helix structure formed by lithium cations is due to the favourable electrostatic interactions with neighbouring phosphorus anions. Further, a theoretical study of $Li_{90}P_{90}$[17] which possesses a circular double-helix structure that resembles the Watson–Crick DNA structure[52] is reported and presented in Figure 9B. NBO analysis of the $Li_{90}P_{90}$ circular double-helix structure shows that the bonding between lithium and phosphorus atoms is quite ionic with effective atomic charges ranging from −0.4 to −0.8 |e| on P. Additionally, NBO analysis revealed the presence of 90 P–P σ-bonds with occupation numbers (ON) equal to 1.92–1.95 |e|, and two lone pairs of *s*- and *p*-type on each phosphorus atom with ONs ranging from 1.72 to 1.84 |e|. The results of the AdNDP analysis are in excellent agreement with the NBO results (Figure 9C).

We next provide evidence that the ET of phosphorous into sulfur indeed occurs in these structures. In Li_xP_x (x = 7–9, 90), the interaction between Li and P atoms are all ionic, and the P atoms obtain enough negative charge to transmutate into S. The electronic configurations of P^- and S are $[Ne]3s^23p^4$, indicating that there should be one *s*- lone pair, one *p*- lone pair, and two *p*- unpaired electrons. Therefore compounds with two σ-bonds formed by these two *p*- unpaired electrons can be expected. It is indeed the case in Li_xP_x (x = 7–9, 90), where each P atom forms two σ-bonds with adjacent two other P atoms and P_n chain structures are observed. However, there are many kinds of sulfur allotropes[42] including various chain and ring structures. The S atoms in these allotropes also possess two σ bonds formed with adjacent two other S atoms. In 2013, Fujimori et al.[53] synthesized single chains of sulfur encapsulated in carbon nanotubes and characterized them with transmission electron microscopy (Figure 9D). Due to the confinement of the nanotube, the sulfur atoms can grow in a single long chain and do not form ring structures. This discovery justifies the ET

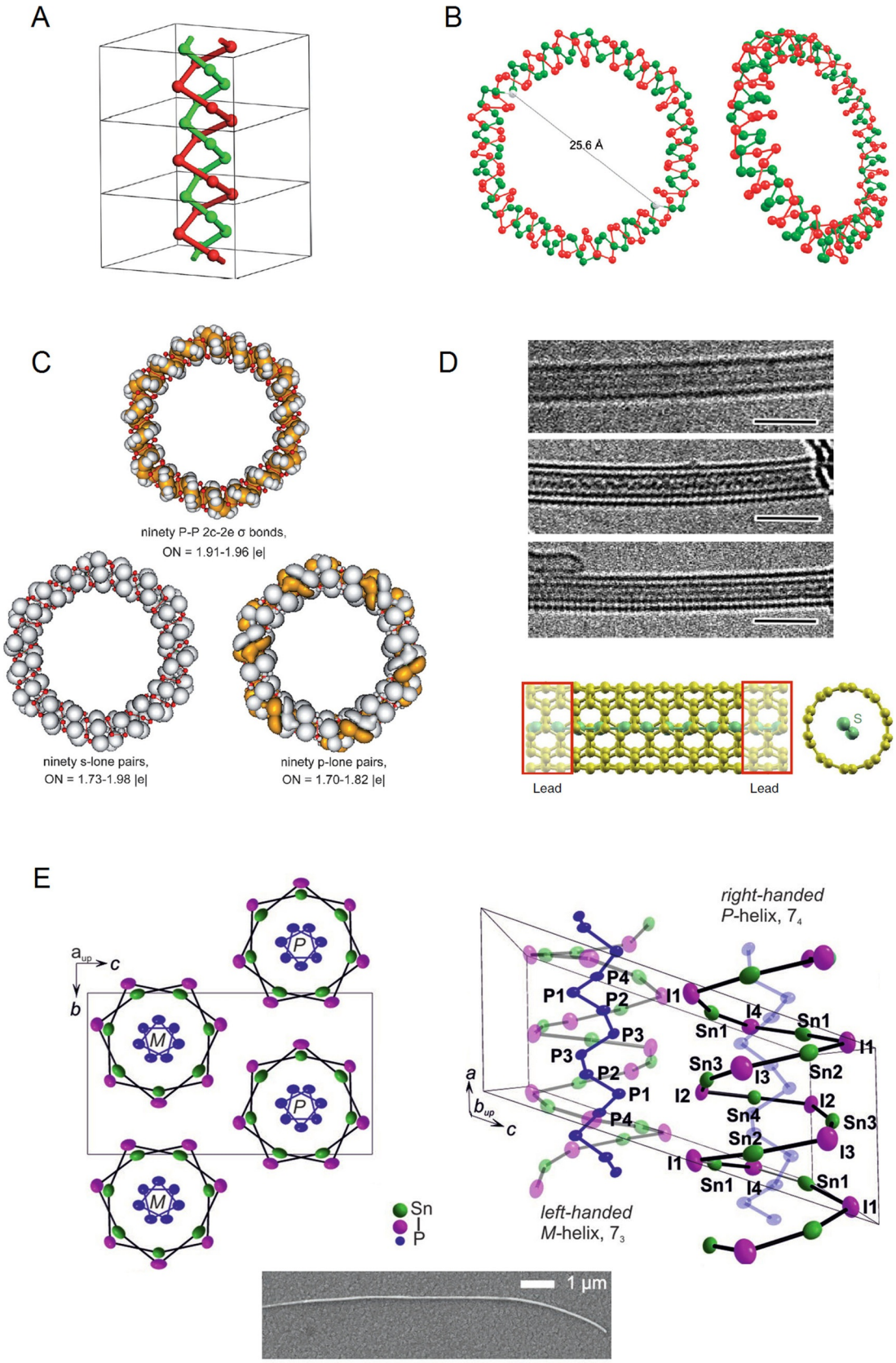

Figure 9. Periodic repetitions of the LiP infinite double-helix chain geometry (A, P in green, Li in red), optimized $Li_{90}P_{90}$ double-helical toroid structure with internal diameter of 25.6 Å (B, P in green, Li in red), chemical bonding pattern of $Li_{90}P_{90}$ shown by the AdNDP analysis (C), the high resolution transmission electron microscopy images and graphical representation of single-walled or double-walled carbon nanotubes encapsulated sulfur chains (D), and crystal structure sections projected along the *a* and *b* axis of SnIP, as well as the scanning electron microscopy (SEM) image of exfoliated SnIP (E).

of phosphorous presented in Figure 9A. In view of this confined S-chain, the Li_nP_n chain inside a carbon nanotube channel was also calculated.[18] More recently, first-principles investigations of a series of inorganic double helical XY (X = Li, Na, K, Rb, Cs; Y = P, As, Sb) structures were conducted.[54] Remarkably, the inorganic double helical SnIP semiconductors containing one [SnI] helix and one [P] helix were synthesized by Nilges and co-workers in the solid state (Figure 9E).[55] The Sn atoms in this material function as the electron donor, and both I and P acquire significant negative charges from Sn. Consistent with the ET principle, it is the negative charge that makes the $[P^-]_\infty$ chain resemble the sulfur chain.

Outlook

The major development of the ET concept has been in silico, where the unbiased global minimum search and the chemical bonding analysis play major roles. The advent of modern gas-phase and solid-state synthesis and characterization techniques greatly helps to identify the ET compounds and justify the ET concept. The main spirit of ET is to discover new exotic compounds and chemical bonding. In the near future, we anticipate that more experimental discoveries of electronically transmutated compounds can be achieved. For example, the $LiAlH_4$ and $LiBH_4$ salts are currently commercially available, and they can be viewed as SiH_4 and CH_4 analogues. We think the large-scale synthesis of $Li_nAl_nH_{2n+2}$, $Li_nB_nH_{2n+2}$ and $Li_nAl_nH_{2n}$ can come true soon since $Li_2Al_3H_8^-$ [8] and $LiAl_2H_4^-$ [9] are observed in the gas phase through the recombination of the plasma generated from the laser vaporization of $LiAlH_4$ powder.

Another concept, the double electronic transmutation (DET) could play a major role in the near future. By acquiring two electrons, a certain element with the atomic number Z could behave similarly as the element Z+2. Based on DET, further examples of transmutation such as B to N, Al to P, C to O is anticipated.

Acknowledgements

This material is based upon work supported by the Air Force Office of Scientific Research (AFOSR) under Grant No. FA9550-15-1-0259 (K.H.B.). The theoretical work was supported by the National Science Foundation (CHE-1664379 to A.I.B). X.Z. acknowledges the Thousand Talents Program of China for Distinguished Young Scholars and the College of Chemistry at Nankai University for the start funding.

Conflict of interest

The authors declare no conflict of interest.

Keywords: anions · chemical bonding · electronic transmutation · global minimum · photoelectron spectroscopy

[1] a) M. Moteki, S. Maeda, K. Ohno, *Organometallics* **2009**, *28*, 2218; b) A. S. Ivanov, A. I. Boldyrev, *J. Phys. Chem. A* **2012**, *116*, 9591.
[2] J. K. Olson, A. I. Boldyrev, *Chem. Phys. Lett.* **2012**, *523*, 83.
[3] A. N. Alexandrova, K. A. Birch, A. I. Boldyrev, *J. Am. Chem. Soc.* **2003**, *125*, 10786.
[4] J. J. Torres-Vega, A. Vásquez-Espinal, M. J. Beltran, L. Ruiz, R. Islas, W. Tiznado, *Phys. Chem. Chem. Phys.* **2015**, *17*, 19602.
[5] J. Poater, M. Solá, C. Viñas, F. Teixidor, *Angew. Chem. Int. Ed.* **2014**, *53*, 12191; *Angew. Chem.* **2014**, *126*, 12387.
[6] J. Nagamatsu, N. Nakagawa, T. Muranaka, Y. Zenitani, J. Akimitsu, *Nature* **2001**, *410*, 63.
[7] J. T. Gish, I. A. Popov, A. I. Boldyrev, *Chem. Eur. J.* **2015**, *21*, 5307.
[8] I. A. Popov, X. Zhang, B. W. Eichhorn, A. Boldyrev, K. H. Bowen, *Phys. Chem. Chem. Phys.* **2015**, *17*, 26079.
[9] K. A. Lundell, X. Zhang, K. H. Bowen, A. I. Boldyrev, *Angew. Chem. Int. Ed.* **2017**, *56*, 16593 – 16596; *Angew. Chem.* **2017**, *129*, 46820 – 16823.
[10] H. Fahlquist, D. Noréus, *Inorg. Chem.* **2013**, *52*, 7125.
[11] H. Fahlquist, D. Noréus, M. H. Sorby, *Inorg. Chem.* **2013**, *52*, 4771.
[12] H. Fahlquist, D. Noréus, S. Callear, W. I. F. David, B. C. Hauback, *J. Am. Chem. Soc.* **2011**, *133*, 14574.
[13] B. H. Boo, S.-J. Kim, M. H. Lee, N. Nishi, *Chem. Phys. Lett.* **2008**, *453*, 150.
[14] N. Perez-Peralta, A. I. Boldyrev, *J. Phys. Chem. A* **2011**, *115*, 11551.
[15] a) G. Auffermann, Y. Prots, R. Kniep, *Angew. Chem. Int. Ed.* **2001**, *40*, 547; *Angew. Chem.* **2001**, *113*, 565; b) G. V. Vajenine, G. Auffermann, Y. Prots, W. Schnelle, R. K. Kremer, A. Simon, R. Kniep, *Inorg. Chem.* **2001**, *40*, 4866; c) S. B. Schneider, R. Frankovsky, W. Schnick, *Angew. Chem. Int. Ed.* **2012**, *51*, 1873; *Angew. Chem.* **2012**, *124*, 1909; d) J. K. Olson, A. S. Ivanov, A. I. Boldyrev, *Chem. Eur. J.* **2014**, *20*, 6636.
[16] A. S. Ivanov, A. J. Morris, K. V. Bozhenko, C. J. Pickard, A. I. Boldyrev, *Angew. Chem. Int. Ed.* **2012**, *51*, 8330; *Angew. Chem.* **2012**, *124*, 8455.
[17] A. S. Ivanov, A. I. Boldyrev, G. Frenking, *Chem. Eur. J.* **2014**, *20*, 2431.
[18] A. S. Ivanov, T. Kar, A. I. Boldyrev, *Nanoscale* **2016**, *8*, 3454.
[19] a) X. Zhang, K. H. Bowen, *J. Chem. Phys.* **2016**, *144*, 224311; b) D. M. P. Mingos, *Nat. Phys. Sci.* **1972**, *236*, 99; c) K. Wade, *Adv. Inorg. Chem. Radiochem.* **1976**, *18*, 1; d) R. E. Williams, *Chem. Rev.* **1992**, *92*, 177; e) R. B. King, D. H. Rouvray, *J. Am. Chem. Soc.* **1977**, *99*, 7834; f) J. J. Aihara, *J. Am. Chem. Soc.* **1978**, *100*, 3339.
[20] a) A. Grubisic, X. Li, S. T. Stokes, J. Cordes, G. F. Ganteför, K. H. Bowen, B. Kiran, P. Jena, R. Burgert, H. Schnöckel, *J. Am. Chem. Soc.* **2007**, *129*, 5969; b) X. Li, A. Grubisic, S. T. Stokes, J. Cordes, G. F. Ganteför, K. H. Bowen, B. Kiran, M. Willis, P. Jena, R. Burgert, H. Schnöckel, *Science* **2007**, *315*, 356; c) X. Li, A. Grubisic, K. H. Bowen, A. K. Kandalam, B. Kiran, G. F. Ganteför, P. Jena, *J. Chem. Phys.* **2010**, *132*, 241103; d) B. Kiran, A. K. Kandalam, J. Xu, Y. H. Ding, M. Sierka, K. H. Bowen, H. Schnöckel, *J. Chem. Phys.* **2012**, *137*, 134303; e) B. Kiran, P. Jena, X. Li, A. Grubisic, S. T. Stokes, G. F. Ganteför, K. H. Bowen, R. Burgert, H. Schnöckel, *Phys. Rev. Lett.* **2007**, *98*, 256802; f) C. Dohmeier, C. Robl, M. Tacke, H. Schnöckel, *Angew. Chem. Int. Ed. Engl.* **1991**, *30*, 564; *Angew. Chem.* **1991**, *103*, 594; g) J. Xu, X. Zhang, S. Yu, Y. Ding, K. Bowen, *J. Phys. Chem. Lett.* **2017**, *8*, 2263; h) X. Zhang, H. Wang, G. Ganteför, B. Eichhorn, B. Kiran, K. H. Bowen, *J. Chem. Phys.* **2016**, *145*, 154305; i) V. Fontenot, B. Kiran, X. Zhang, H. Wang, G. Ganteför, K. H. Bowen, *Int. J. Mass Spectrom.* **2016**, *408*, 56; j) H. Wang, X. Zhang, Y. Ko, G. F. Gantefor, K. H. Bowen, X. Li, K. Boggavarapu, A. Kandalam, *J. Chem. Phys.* **2014**, *140*, 164317; k) H. Wang, Y. Ko, X. Zhang, G. Gantefoer, H. Schnoeckel, B. W. Eichhorn, P. Jena, B. Kiran, A. K. Kandalam, K. H. Bowen, *J. Chem. Phys.* **2014**, *140*, 124309; l) H. Wang, X. Zhang, J. Ko, A. Grubisic, X. Li, G. Ganteför, H. Schnöckel, B. Eichhorn, M. Lee, P. Jena, A. Kandalam, B. Kiran, K. H. Bowen, *J. Chem. Phys.* **2014**, *140*, 054301.
[21] a) A. Schnepf, H. Schnöckel, *Angew. Chem. Int. Ed.* **2002**, *41*, 3532; *Angew. Chem.* **2002**, *114*, 3682; b) A. Schnepf, G. Stösser, H. Schnöckel, *J. Am. Chem. Soc.* **2000**, *122*, 9178; c) A. Schnepf, H. Schnöckel, *Angew. Chem. Int. Ed.* **2001**, *40*, 711; *Angew. Chem.* **2001**, *113*, 733; d) H. Schnöckel, *Chem. Rev.* **2010**, *110*, 4125.
[22] P. Laszlo, *Angew. Chem. Int. Ed.* **2000**, *39*, 2071; *Angew. Chem.* **2000**, *112*, 2151.
[23] L. Andrews, X. Wang, *Science* **2003**, *299*, 2049.
[24] A. J. Downs, M. J. Goode, C. R. Pulham, *J. Am. Chem. Soc.* **1989**, *111*, 1936.
[25] a) Y.-R. Luo, Bond Dissociation Energies. In CRC Handbook of Chemistry and Physics, 89th ed.; Lide, D. R., Ed.; CRC Press/Taylorand Francis: Boca Raton, FL, **2009**; b) K. A. Nguyen, K. Lammertsma, *J. Phys. Chem. A* **1998**, *102*, 1608.

[26] A. P. Sergeeva, B. B. Averkiev, H.-J. Zhai, A. I. Boldyrev, L. S. Wang, *J. Chem. Phys.* **2011**, *134*, 224304.
[27] a) A. D. Becke, *J. Chem. Phys.* **1993**, *98*, 5648; b) S. H. Vosko, L. Wilk, M. Nusair, *Can. J. Phys.* **1980**, *58*, 1200; c) C. Lee, W. Yang, R. G. Parr, *Phys. Rev. B* **1988**, *37*, 785; d) J. S. Binkley, J. A. Pople, W. J. Hehre, *J. Am. Chem. Soc.* **1980**, *102*, 939.
[28] a) M. S. Gordon, J. S. Binkley, J. A. Pople, W. J. Pietro, W. J. Hehre, *J. Am. Chem. Soc.* **1982**, *104*, 2797; b) W. J. Pietro, M. M. Francl, W. J. Hehre, D. J. Defrees, J. A. Pople, J. S. Binkley, *J. Am. Chem. Soc.* **1982**, *104*, 5039; c) A. D. McLean, G. S. Chandler, *J. Chem. Phys.* **1980**, *72*, 5639; d) T. Clark, J. Chandrasekhar, G. W. Spitznagel, P.v.R. Schleyer, *J. Comput. Chem.* **1983**, *4*, 294.
[29] a) J. Cizek, *Adv. Chem. Phys.* **1969**, *14*, 35; b) G. Purvis, R. J. Bartlett, *J. Chem. Phys.* **1982**, *76*, 1910; c) K. Raghavachari, G. W. Trucks, J. A. Pople, M. Head-Gordon, *Chem. Phys. Lett.* **1989**, *157*, 479.
[30] a) D. E. Woon, T. H. Dunning Jr, *J. Chem. Phys.* **1993**, *98*, 1358; b) R. A. Kendall, T. H. Dunning, Jr., R. J. Harrison, *J. Chem. Phys.* **1992**, *96*, 6796; c) T. H. Dunning Jr, *J. Chem. Phys.* **1989**, *90*, 1007; d) K. A. Peterson, D. E. Woon, T. H. Dunning Jr, *J. Chem. Phys.* **1994**, *100*, 7410; e) A. Wilson, T. van Mourik, T. H. Dunning Jr, *J. Mol. Struct.* **1996**, *388*, 339.
[31] a) D. G. Truhlar, *Chem. Phys. Lett.* **1998**, *294*, 45; b) P. L. Fast, M. L. Sanchez, D. G. Truhlar, *J. Chem. Phys.* **1999**, *111*, 2921.
[32] D. Yu. Zubarev, A. I. Boldyrev, *Phys. Chem. Chem. Phys.* **2008**, *10*, 5207.
[33] a) Gaussian 03 (Revision D.01), M. J. Frisch, G. W. Trucks, H. B. Schlegel, G. E. Scuseria, M. A. Robb, J. R. Cheeseman, J. A. Montgomery Jr., T. Vreven, K. N. Kudin, J. C. Burant, J. M. Millam, S. S. Iyengar, J. Tomasi, V. Barone, B. Mennucci, M. Cossi, G. Scalmani, N. Rega, G. A. Petersson, H. Nakatsuji, M. Hada, M. Ehara, K. Toyota, R. Fukuda, J. Hasegawa, M. Ishida, T. Nakajima, Y. Honda, O. Kitao, H. Nakai, M. Klene, X. Li, J. E. Knox, H. P. Hratchian, J. B. Cross, C. Adamo, J. Jaramillo, R. Gomperts, R. E. Stratmann, O. Yazyev, A. J. Austin, R. Cammi, C. Pomelli, J. W. Ochterski, P. Y. Ayala, K. Morokuma, G. A. Voth, P. Salvador, J. J. Dannenberg, V. G. Zakrzewski, S. Dapprich, A. D. Daniels, M. C. Strain, O. Farkas, D. K. Malick, A. D. Rabuck, K. Raghavachari, J. B. Foresman, J. V. Ortiz, Q. Cui, A. G. Baboul, S. Clifford, J. Cioslowski, B. B. Stefanov, G. Liu, A. Liashenko, P. Piskorz, I. Komaromi, R. L. Martin, D. J. Fox, T. Keith, M. A. Al-Laham, C. Y. Peng, A. Nanayakkara, M. Challacombe, P. M. W. Gill, B. Johnson, W. Chen, M. W. Wong, C. Gonzalez, J. A. Pople, Gaussian, Inc., Wallingford CT, **2004**.; b) Gaussian 09 (Revision B.01), M. J. Frisch, G. W. Trucks, H. B. Schlegel, G. E. Scuseria, M. A. Robb, J. R. Cheeseman, G. Scalmani, V. Barone, B. Mennucci, G. A. Petersson, H. Nakatsuji, M. Caricato, X. Li, H. P. Hratchian, A. F. Izmaylov, J. Bloino, G. Zheng, J. L. Sonnenberg, M. Hada, M. Ehara, K. Toyota, R. Fukuda, J. Hasegawa, M. Ishida, T. Nakajima, Y. Honda, O. Kitao, H. Nakai, T. Vreven, J. A. Montgomery, Jr., J. E. Peralta, F. Ogliaro, M. Bearpark, J. J. Heyd, E. Brothers, K. N. Kudin, V. N. Staroverov, R. Kobayashi, J. Normand, K. Raghavachari, A. Rendell, J. C. Burant, S. S. Iyengar, J. Tomasi, M. Cossi, N. Rega, J. M. Millam, M. Klene, J. E. Knox, J. B. Cross, V. Bakken, C. Adamo, J. Jaramillo, R. Gomperts, R. E. Stratmann, O. Yazyev, A. J. Austin, R. Cammi, C. Pomelli, J. W. Ochterski, R. L. Martin, K. Morokuma, V. G. Zakrzewski, G. A. Voth, P. Salvador, J. J. Dannenberg, S. Dapprich, A. D. Daniels, Ö. Farkas, J. B. Foresman, J. V. Ortiz, J. Cioslowski, D. J. Fox, Gaussian, Inc. Wallingford CT, **2009**..
[34] U. Varetto, Molekel 5.4.0.8, Swiss National Supercomputing Centre, Manno, Switzerland, **2009**.
[35] MOLDEN 3.4. Schaftenaar, G. MOLDEN3.4, CAOS/CAMM Center, The Netherlands, **1998**.
[36] F. W. McLafferty, J. Winkler, *J. Am. Chem. Soc.* **1974**, *96*, 5182.
[37] a) J. P. Foster, F. Weinhold, *J. Am. Chem. Soc.* **1980**, *102*, 7211; b) A. E. Reed, F. Weinhold, *J. Chem. Phys.* **1983**, *78*, 4066; c) A. E. Reed, R. B. Weinstock, F. Weinhold, *J. Chem. Phys.* **1985**, *83*, 735.
[38] a) P. v. R. Schleyer, C. Maerker, A. Dransfeld, H. Jiao, N. J. R. v. E. Hommes, *J. Am. Chem. Soc.* **1996**, *118*, 6317; b) P. v. R. Schleyer, H. Jiao, N. J. R. v. E. Hommes, V. G. Malkin, O. L. Malkina, *J. Am. Chem. Soc.* **1997**, *119*, 12669; c) P. v. R. Schleyer, K. Najafian, *Inorg. Chem.* **1998**, *37*, 3454.
[39] A. Geim, *Science* **2009**, *324*, 1530.
[40] W. Li, L. Kong, C. Chen, J. Gou, S. Sheng, W. Zhang, H. Li, L. Chen, P. Cheng, K. Wu, *Sci. Bull.* **2018**, *63*, 282 – 286.
[41] B. Feng, J. Zhang, Q. Zhong, W. Li, S. Li, H. Li, P. Cheng, S. Meng, L. Chen, K. Wu, *Nat. Chem.* **2016**, *8*, 563.
[42] W. W. Porterfield, *Inorganic Chemistry: A Unified Approach*, Academic Press, San Diego (USA), **1993**.
[43] J. D. Graham, A. M. Buytendyk, X. Zhang, E. L. Collins, K. Boggavarapu, G. Gantefoer, B. W. Eichhorn, G. L. Gutsev, S. Behera, P. Jena, K. H. Bowen, *J. Phys. Chem. A* **2014**, *118*, 8158.
[44] X. Zhang, Y. Wang, H. Wang, A. Lim, G. Ganteför, K. H. Bowen, J. U. Reveles, S. N. Khanna, *J. Am. Chem. Soc.* **2013**, *135*, 4856.
[45] J. Ho, K. M. Ervin, W. C. Lineberger, *J. Chem. Phys.* **1990**, *93*, 6987.
[46] P. Bag, A. Porzelt, P. J. Altmann, S. Inoue, *J. Am. Chem. Soc.* **2017**, *139*, 14384.
[47] S. Bonyhady, J. N. Holzmann, G. Frenking, A. Stasch, C. Jones, *Angew. Chem. Int. Ed.* **2017**, *56*, 8527.
[48] I. B. Bersuker, *Chem. Rev.* **2013**, *113*, 1351.
[49] G. Grzybowski, L. Jiang, R. T. Beeler, T. Watkins, A. V. G. Chizmeshya, C. Xu, J. Menéndez, J. Kouvetakis, *Chem. Mater.* **2012**, *24*, 1619.
[50] R. Nesper, *Z. Anorg. Allg. Chem.* **2014**, *640*, 2639.
[51] a) L. A. Stearns, J. Gryko, J. Diefenbacher, G. K. Ramachandran, P. F. McMillan, *J. Solid State Chem.* **2003**, *173*, 251; b) J. Evers, G. Oehlinger, G. Sextl, *Angew. Chem. Int. Ed. Engl.* **1993**, *32*, 1442; *Angew. Chem.* **1993**, *105*, 1532.
[52] J. D. Watson, F. H. C. Crick, *Nature* **1953**, *171*, 737.
[53] T. Fujimori, A. Morelos-Gómez, Z. Zhu, H. Muramatsu, R. Futamura, K. Urita, M. Terrones, T. Hayashi, M. Endo, S. Y. Hong, Y. C. Choi, D. Tománek, K. Kaneko, *Nat. Commun.* **2013**, *4*, 2162.
[54] W. Ju, H. Wang, T. Li, H. Liu, H. Han, *RSC Adv.* **2016**, *6*, 50444.
[55] D. Pfister, K. Schäfer, C. Ott, B. Gerke, R. Pöttgen, O. Janka, M. Baumgartner, A. Efimova, A. Hohmann, P. Schmidt, S. Venkatachalam, L. van Wüllen, U. Schürmann, L. Kienle, V. Duppel, E. Parzinger, B. Miller, J. Becker, A. Holleitner, R. Weihrich, T. Nilges, *Adv. Mater.* **2016**, *28*, 9783.

Manuscript received: February 1, 2018
Accepted manuscript online: March 8, 2018
Version of record online: April 19, 2018